Novel Extended Robust Disturbance Observer for Improved Cogging Force Compensation in Permanent Magnet Linear Motors

Franz Luckert*, Axel Mertens**
WITTENSTEIN cyber motor GmbH
97999 Igersheim, Germany
Phone: +49 (0) 7931 493-18050
Fax: +49 (0) 7931 493-200
Email: franz.luckert@wittenstein.de
URL: https://www.cyber-motor.wittenstein.de/

**Institute for Drive Systems and Power Electronics
Leibniz University Hannover
30167 Hannover, Germany
Phone: +49 (0) 511 762-2471
Fax: +49 (0) 511 762-3040
Email: mertens@ial.uni-hannover.de
URL: https://www.ial.uni-hannover.de

Keywords

≪Linear drive≫, ≪Ripple minimization≫, ≪Neural network≫, ≪Industrial application≫, ≪Robust control≫

Abstract

This paper presents an extended robust disturbance observer for improved force ripple compensation of a permanent magnet synchronous linear motor. In extension, working from the output of the robust disturbance observer, the amplitudes of dominant harmonics are estimated by means of a harmonic-activated neural network. With the knowledge of the amplitude, the phase shift of an individual harmonic resulting from the robust disturbance observer can be corrected. This method improves the cogging force compensation by feedforward, especially when the frequency of the force ripple increases due to higher travelling speeds.

Introduction

Numerous industrial applications require linear motion with high demands on dynamic and positioning accuracy [1]. These include wafer scanners and wafer steppers used for photolithography in the manufacture of semiconductors. While wafer steppers have strict accuracy requirements regarding the final position of their movement, wafer scanners require a high positioning accuracy during their constant movement [2]. A drive that is ideally suited for linear positioning tasks is the permanent magnet synchronous linear motor (PMSLM). The PMSLM is a direct drive with high dynamics and virtually unlimited positioning range. However, its design leads to a force ripple, which has a detrimental effect on the positioning accuracy in the micrometer range.
Many efforts have already been made to reduce the cogging force of linear motors. In addition to design approaches, different control strategies have been investigated. A feedforward compensation based on offline determination of the cogging force was presented in [3]. However, due to manufacturing tolerances, the experimental determination of the first-order ripple forces must be performed for each

PMSLM individually. For this reason, the concept would be very costly for broad application. In [4], a neural-network-based feedforward-assisted feedback controller was investigated. [5] presents a disturbance observer based on an inverse model of the plant. Because of a lack of inhibiting ability for middle- and high-frequency force ripple components, the proposed disturbance observer cannot compensate force ripple completely. To deal with the higher harmonics of the cogging force, a compensation method based on inverse model iterative learning in combination with a robust disturbance observer (RDOB) is investigated in [6]. Neural networks for an inversion based feedforward controller design were investigated in [9]. While neural networks with an autoregressive exogeneous structure were not able to improve tracking performance due to being unable to track the general system dynamics, physicsguided neural networks increase performance compared to several other benchmark feedforward strategies like, for example, massacceleration feedforward. A force ripple compensation strategy using a fuzzy-adaptive Kalman filter was investigated in [10]. The fuzzy-adaptive Kalman filter algorithm is able to reduce the effort needed to estimate the noise covariance matrix by tuning the parameters. Due to the improved noise reduction, the force ripple and, thus, also the position tracking performance is significantly improved.

This paper is based on the RDOB detailed in [6]. The focus is placed on extending the RDOB to minimize the effect of phase shift at higher harmonics of the cogging force. Finally, an extended robust disturbance observer (ERDOB) is presented that is able to suppress the dominant higher harmonic components of the cogging force. For this purpose, the amplitudes of the dominant harmonic components are estimated by means of a harmonic-activated neural network (HANN). By knowing amplitudes of the dominant harmonics and position of the moving part, these components of the cogging force can be canceled by feedforward control.

This paper is divided into three sections. First, the problem is described and the underlying model is explained. Second, the structure of the ERDOB is presented and this is finally verified by experiments in the last section.

Modeling and problem description

The model of the PMSLM is known from the literature [4]. Since the current control loop is assumed to be fast enough, only the mechanical dynamics of the PMSLM are considered:

$$\ddot{x}(t) = \frac{f_{\mathrm{i}}(i_{\mathrm{q}},t) - f_{\mathrm{f}}(\dot{x},t) - f_{\mathrm{c}}(x,t)}{m}. \tag{1}$$

$$\text{with } f_{\mathrm{i}}(i_{\mathrm{q}},t) = k_{\mathrm{F}} \cdot i_{\mathrm{q}}(t). \tag{2}$$

The parameter m represents the mass of the glider. k_{F} is the force constant of the PMSLM and i_{q} is the current in the q-axis. x denotes the position of the glider and $\ddot{x}$ is its acceleration. Furthermore, the model contains the speed-dependent frictional force f_{f} and the position-dependent cogging force f_{c}, which are understood to be disturbance forces:

$$f_{\mathrm{d}}(x,\dot{x},t) = f_{\mathrm{f}}(\dot{x},t) + f_{\mathrm{c}}(x,t). \tag{3}$$

As already mentioned, the cogging force is caused by the mechanical design of the PMSLM. Parameters such as the opening of the stator slots or the finite length of the glider generate spatially distributed periodic disturbance forces. According to [8], the cogging force can finally be modeled as a Fourier series expansion truncated after the N-th harmonic:

$$f_{\mathrm{c}}(x,t) \quad = \quad F_0 + \sum_{n=1}^{\mathrm{N}} F_{\mathrm{cA},n} \cdot \cos\left(\frac{\pi}{\tau_{\mathrm{P}}} \cdot k_{\mathrm{c},n} \cdot x(t)\right) + \sum_{n=1}^{\mathrm{N}} F_{\mathrm{cB},n} \cdot \sin\left(\frac{\pi}{\tau_{\mathrm{P}}} \cdot k_{\mathrm{c},n} \cdot x(t)\right). \tag{4}$$

Here, $k_{\mathrm{c},n}$ denotes the period of the n-th harmonic of the cogging force as a multiple of the pole pitch τ_{P}. The parameters $F_{\mathrm{cA},n}$ and $F_{\mathrm{cB},n}$ describe the amplitudes of the even and odd parts of the harmonic.

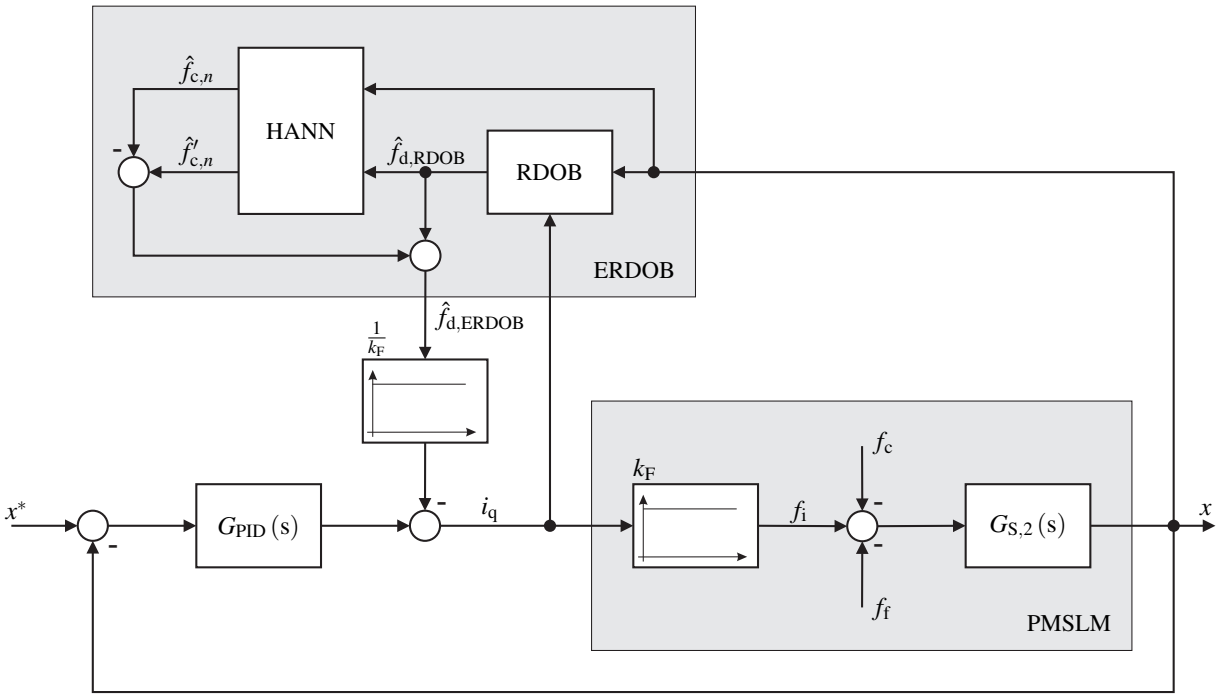

Fig. 1: The structure of the controlled system

Design of the extended robust disturbance observer

The ERDOB combines an RDOB and a HANN to minimize the effect of cogging force on the positionalaccuracy by using feedforward control. The structure of the control system is shown in Figure 1. The RDOB estimates the disturbance forces from the measured position x and known control value i_q. For this purpose, the positional value is multiplied with the inverse transfer function of the disturbance. Since the inverse plant model is double differentiating, it is multiplied by a second-order low-pass filter to make it proper and to obtain a practically realizable transfer function for the RDOB:

$$G_{RDOB}(s) = G_{S,2}^{-1}(s) \cdot G_{LP}(s) = \frac{m \cdot s^2}{\xi_2 \cdot s^2 + \xi_1 \cdot s + \xi_0}. \tag{5}$$

The parameters ξ_0, ξ_1, ξ_2 are the coefficients of the low-pass filter. In Equation (1), it can be seen that not only the disturbance forces f_c and f_f, but also the control value f_i, affect the output x of the plant. To obtain solely the disturbance forces, the low-pass filtered control value f_i must be subtracted from the output of $G_{RDOB}(s)$:

$$\hat{F}_{d,RDOB}(s) = \hat{F}_{c,RDOB}(s) + \hat{F}_{f,RDOB}(s) = G_{RDOB}(s) \cdot X(s) - k_F \cdot G_{LP}(s) \cdot I_q(s). \tag{6}$$

$\hat{F}_{d,RDOB}(s)$, $\hat{F}_{c,RDOB}(s)$, $\hat{F}_{f,RDOB}(s)$, $X(s)$ and $I_q(s)$ denote the Laplace transformation of these variables. The final results are the estimated frictional force $\hat{f}_{f,RDOB}$ and the estimated cogging force $\hat{f}_{c,RDOB}$. In terms of estimating the cogging force, however, this robust disturbance force observer also has a distinct disadvantage. As already described at the beginning, the cogging force consists of several harmonics. Depending on their order and the speed of the glider, the estimated harmonics are phase shifted. As a result, these cannot be completely canceled out by feedforward control.

$\hat{F}_{d,RDOB}(s)$, $\hat{F}_{c,RDOB}(s)$, $\hat{F}_{f,RDOB}(s)$, $X(s)$ and $I_q(s)$ denote the Laplace transformation of these variables. The result is finally the estimated friction force $\hat{f}_{f,RDOB}$ and the estimated cogging force $\hat{f}_{c,RDOB}$. In terms of estimating the cogging force, however, this robust disturbance force observer also has a decisive disadvantage. As already described at the beginning, the cogging force consists of several harmonics. Depending on their order and the speed of the glider, the estimated harmonics are phase shifted. As a

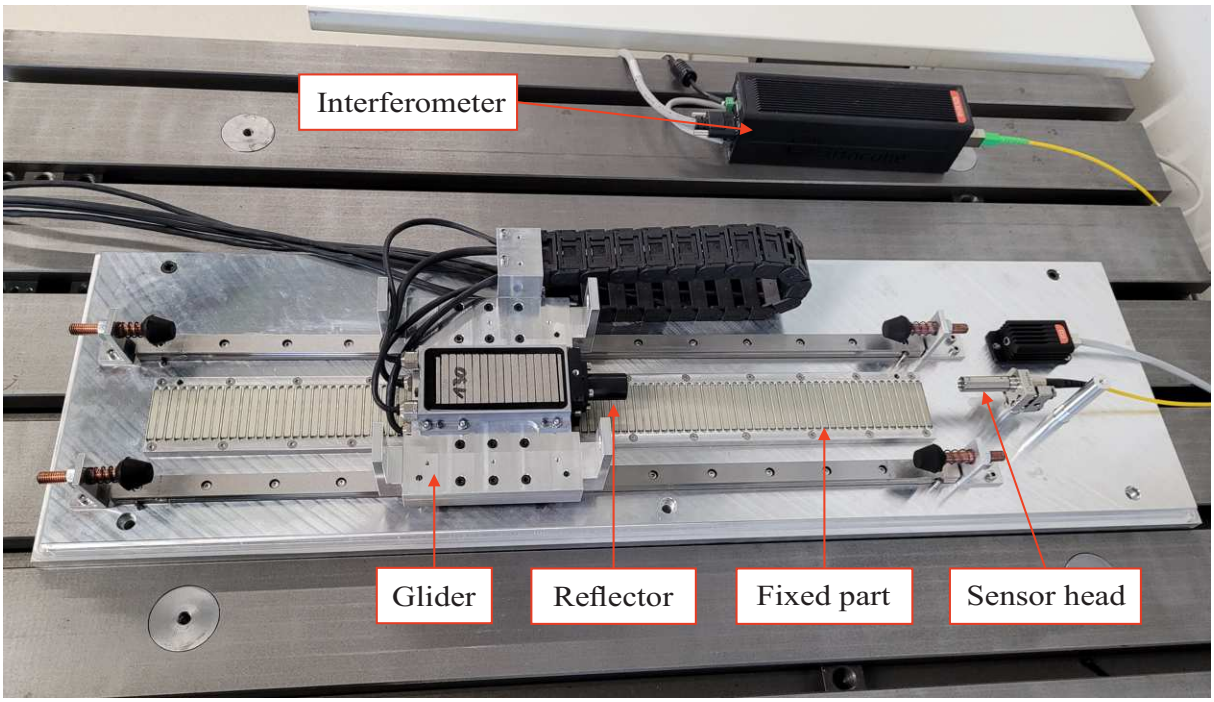

Fig. 2: The test setup for experimental investigation

result, these cannot be completely canceled out by feedforward control.

By performing an FFT on the positional error, the remaining influence of each harmonic can be determined. To improve the cogging force estimation, dominant harmonics can be canceled by feedforwarding them in the correct phase position. As the order of the desired harmonic is already known, only the amplitude and phase are needed. For estimating these two parameters, a HANN presented in [7] is used. The neural network for the desired harmonic is modeled according to Equation (4):

$$\hat{f}_{\mathrm{c},n}(x,t) = \hat{\Theta}_{\mathrm{A},n}(t) \cdot \sin\left(\frac{\pi}{\tau_\mathrm{P}} \cdot k_{\mathrm{c},n} \cdot x(t)\right) + \hat{\Theta}_{\mathrm{B},n}(t) \cdot \cos\left(\frac{\pi}{\tau_\mathrm{P}} \cdot k_{\mathrm{c},n} \cdot x(t)\right) \tag{7}$$

$$\text{with } \hat{\Theta}_{\mathrm{A},n}(t=0) = \hat{\Theta}_{\mathrm{A0},n},\ \hat{\Theta}_{\mathrm{B},n}(t=0) = \hat{\Theta}_{\mathrm{B0},n}. \tag{8}$$

The index n denotes the order of the harmonic to be estimated. $\hat{\Theta}_{\mathrm{A},n}$ and $\hat{\Theta}_{\mathrm{B},n}$ are the amplitudes of its even and odd spectral components. For calculating the error, the previously estimated cogging force of the RDOB is used:

$$e(t) = \hat{f}_{\mathrm{c,n}}(x,t) - \hat{f}_{\mathrm{d,RDOB}}(x,t). \tag{9}$$

In principle, the error could also be calculated from the measured position, as with the RDOB. But in this case, the cogging force would pass through the strictly positive real transfer function $G_{\mathrm{S},2}(s)$ of the plant, which would require a more complex error network. In order to adapt the amplitudes $\hat{\Theta}_\mathrm{A}$ and $\hat{\Theta}_\mathrm{B}$, a gradient descent method is used as the learning law:

$$\frac{\mathrm{d}}{\mathrm{dt}}\hat{\Theta}_{\mathrm{A},n}(t) = -\eta \cdot e(t) \cdot \sin\left(\frac{\pi}{\tau_\mathrm{P}} \cdot k_{\mathrm{c},n} \cdot x(t)\right) \tag{10}$$

$$\frac{\mathrm{d}}{\mathrm{dt}}\hat{\Theta}_{\mathrm{B},n}(t) = -\eta \cdot e(t) \cdot \cos\left(\frac{\pi}{\tau_\mathrm{P}} \cdot k_{\mathrm{c},n} \cdot x(t)\right). \tag{11}$$

Here, η denotes the increment of the learning law. Finally, the HANN provides the amplitudes of the even and odd components of the n-th harmonic of the previously estimated and phase-shifted cogging

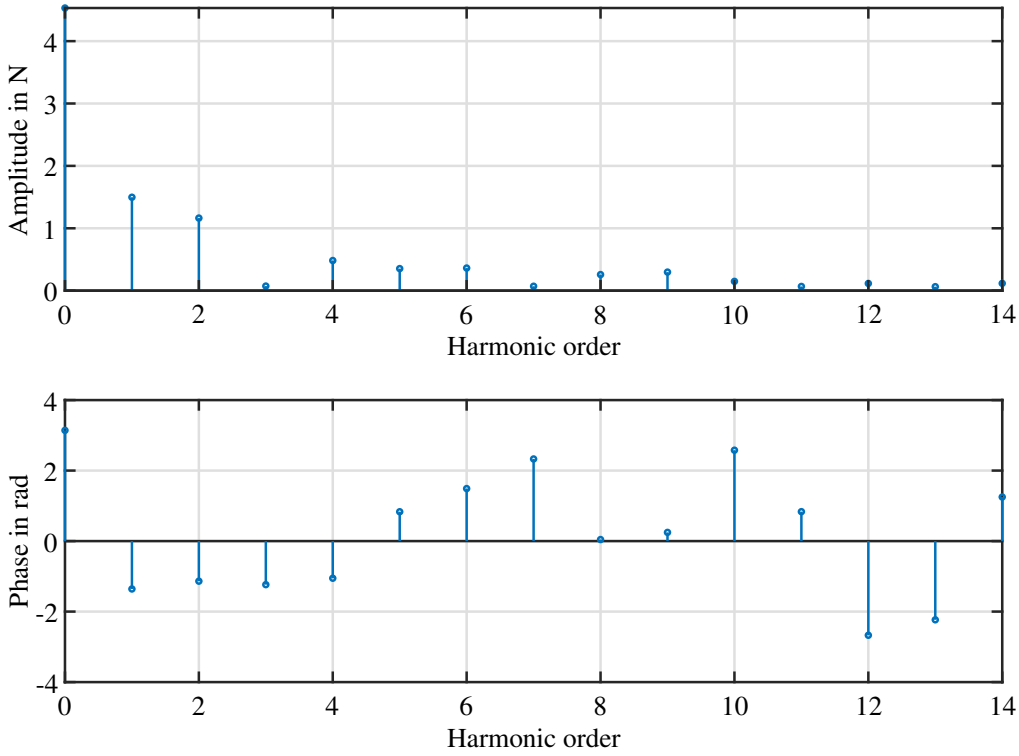

Fig. 3: Estimated disturbance force frequency characteristic

force $\hat{f}_{\mathrm{c,RDOB}}$. Due to the fact that the frequency of the harmonic is known from its period $k_{c,n}$ and the glider speed $\dot{x}$, the phase shift $\varphi_{\mathrm{LP},n}$ caused by the low-pass filter can be calculated and corrected:

$$\hat{f}'_{\mathrm{c},n}(x,t) = \hat{\Theta}_{\mathrm{A},n}(t) \cdot \cos\left(\frac{\pi}{\tau_{\mathrm{P}}} \cdot k_{\mathrm{c},n} \cdot x(t) - \varphi_{\mathrm{LP},n}\right) + \hat{\Theta}_{\mathrm{B},n}(t) \cdot \sin\left(\frac{\pi}{\tau_{\mathrm{P}}} \cdot k_{\mathrm{c},n} \cdot x(t) - \varphi_{\mathrm{LP},n}\right). \tag{12}$$

Finally, the estimated disturbance force of the ERDOB is the calculated:

$$\hat{f}_{\mathrm{d,ERDOB}}(x,t) = \hat{f}_{\mathrm{d,RDOB}}(x,t) - \hat{f}_{\mathrm{c},n}(x,t) + \hat{f}'_{\mathrm{c},n}(x,t). \tag{13}$$

The estimated disturbance force can be used to compensate the force ripple by feedforward control. The validation of this concept will be presented in the next section.

Experimental results

To demonstrate the effectiveness of the proposed ERDOB, it is now validated by experiment. The experimental setup shown in Figure 2 uses a standard WITTENSTEIN PMSLM, which is not optimized for low cogging force. It is equipped with an Attocube interferometer providing a positional resolution of 1 nm. The newly designed control algorithm is implemented on a dSPACE rapid prototyping system with the DS1006 processor board, which has a sampling rate of 16 kHz.
In the first step, the plant of the experimental setup is analyzed and the dominant harmonics of the disturbance force are determined. In the second step, it is considered how well these can be suppressed by using the ERDOB.

Identification of the disturbance forces and system analysis

To determine the disturbance force, the glider is moved at a very low speed of 0.01 m/s by PID control. If we now apply an FFT to the output signal $\hat{f}_{\mathrm{d,RDOB}}$ of the RDOB, we obtain the spectrum of the estimated

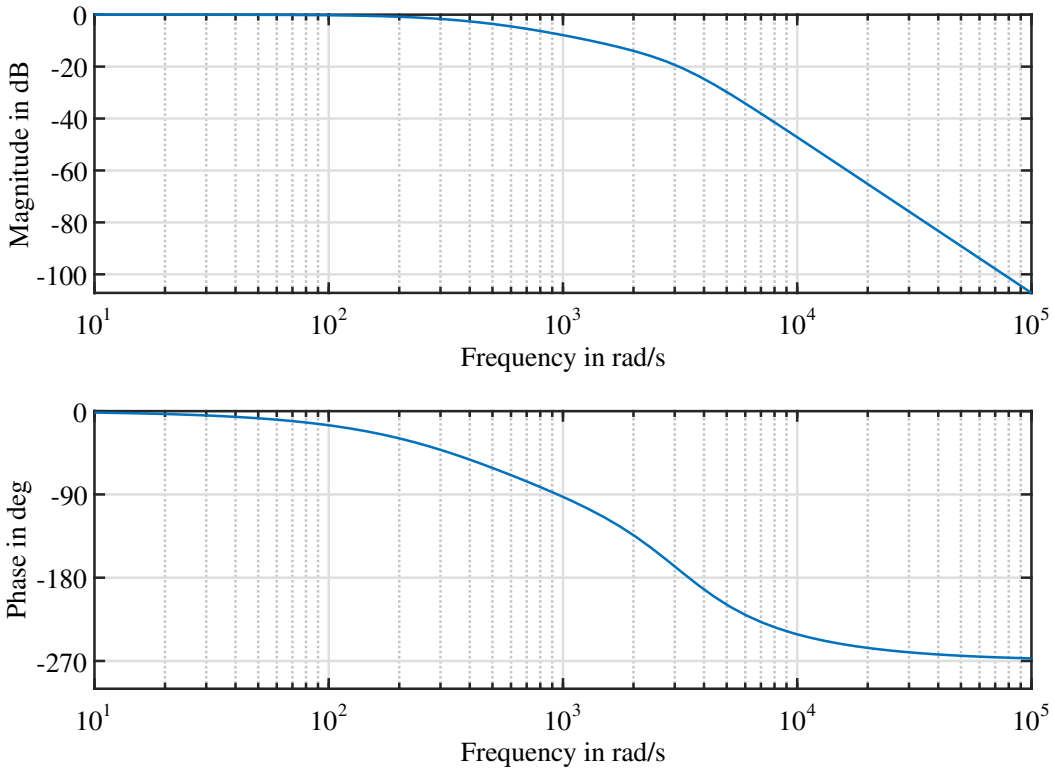

Fig. 4: Bode plot of the RDOB

disturbance force. The parameters of the RDOB are chosen to be $\xi_0 = 1$, $\xi_1 = 0.45\,\mathrm{ms}$, $\xi_2 = 0.1\,\mathrm{ms}^2$. The time constant for the additional low-pass filter is $T_{\mathrm{LP}} = 1.59\,\mathrm{ms}$. Since the transfer functions of $G_{\mathrm{LP},1}(s)$ and $G_{\mathrm{LP},2}(s)$ are known, the amplitudes of the single harmonics together with their phase shifts can finally be corrected. The results are shown in Figure 3. Beside the frictional force, the two harmonics with order $k_{\mathrm{c},1} = 1$ and $k_{\mathrm{c},2} = 2$ are dominant. The Bode plot of the RDOB in Figure 4 shows that a phase shift is already occurring for the first-order harmonic at a speed $v = 0.1\,\mathrm{m/s}$, which results in a frequency of $\omega_{\mathrm{c},1} = 57\,\mathrm{rad/s}$. For the second-order harmonic, attenuation is already taking effect. Since the frequency increases proportional to the velocity, phase correction should already be applied to the first-order and second-order harmonics. The effect of these will be investigated in the next section.

Measurement

To evaluate the benefits of amplitude and phase corrections, the ERDOB is compared to a system in which the cogging force for feedforward control is estimated by using only the RDOB. The results are also compared to a system without cogging force feedforward, which is only PID controlled. For the investigation, a trapezoidal velocity profile is used and the glider is moved over a distance of 100 mm at a constant speed. For the system with cogging force estimation and feedforward control, a settling time of 0.1 s is allowed, after which the remaining positional error $\Delta x = x - x^*$ is then determined.
The HANN of the ERDOB is set up to estimate the two dominant harmonics $k_{\mathrm{c},1} = 1$ and $k_{\mathrm{c},2} = 2$ of the cogging force determined when analyzing the plant. For this purpose, the increment of the learning law is chosen to be $\eta = 50$.
Figure 5 a) shows the remaining positional error for a constant glider speed of $v = 0.1\,\mathrm{m/s}$. The maximum positional error for the PID-controlled system is 4.503 μm. By feedforwarding the disturbance force estimated with the RDOB, the remaining positional error can be limited to 1.543 μm after the settling period. If the cogging force estimated with the proposed ERDOB is used for cogging force cancelation, the positional error can be reduced to 1.117 μm. Finally, the spectrum of the resulting positional error is shown in Figure 5 b). As can be seen here, the ERDOB does not have any impact on the

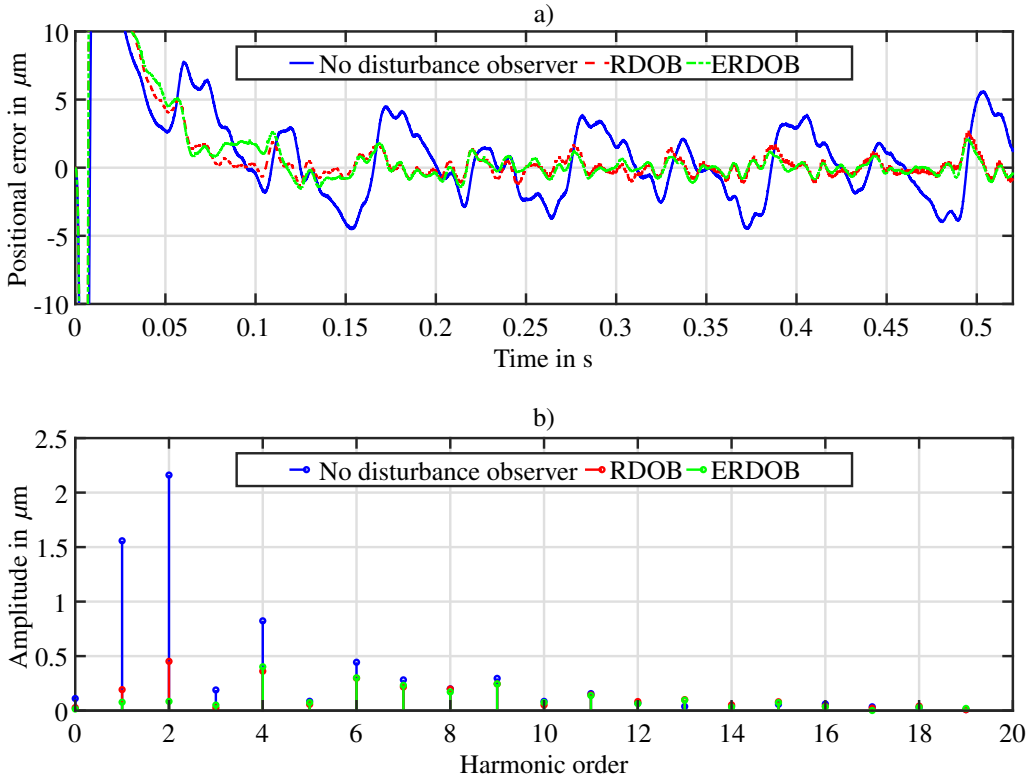

Fig. 5: a) Positional error for $v = 0.1\,\mathrm{m/s}$; b) Positional error frequency characteristic for $v = 0.1\,\mathrm{m/s}$

first-order harmonic of the cogging force compared to the RDOB. But it is able to reduce the impact of the second-order harmonic of the cogging force on the positional error.

Figure 6 a) shows the remaining positional error for the glider moving at a constant speed of $v = 0.2\,\mathrm{m/s}$. The maximum positional error for the PID-controlled system is 5.152 μm. By feedforwarding the disturbance force estimated with the RDOB, the remaining positional error can be limited to 3.403 μm after the settling period. By using the proposed ERDOB for cogging force estimation, the positional error can be reduced to 2.562 μm. Even at the speed $v = 0.2\,\mathrm{m/s}$, the ERDOB was able to reduce the second-order harmonic in the positional error by suppressing the cogging force, as Figure 6 b) shows. The impact on the first-order harmonic is still very low as this is compensated well enough by the RDOB itself, due to low phase shift and low attenuation.

Lastly, a travelling speed of $v = 0.5\,\mathrm{m/s}$ is considered. With this movement, the PID controller can only limit the positional deviation to 4.590 μm. If the disturbance forces, which are only estimated with the RDOB, are feedforward, the positional error after the settling period can be limited to 3.797 μm. By using the proposed ERDOB, the remaining positional error is only 2.3 μm. The results are shown in Figure 7 a). With the increased speed, the phase correction of the ERDOB becomes more important. Figure 7 b) shows that the RDOB is no longer able to suppress the second-order harmonic of the cogging force. But with the ERDOB, it can be reduced as well as the first-order harmonic by using the ERDOB appropriately.

The experiments have shown that the positional error can be reduced by using a disturbance observer. If no observer is used to suppress the harmonics of the cogging force, the positional error remains in the same range for all three glider speeds considered. With higher glider velocities, the positional error for the feedforward control with the RDOB increases together with the phase shift and attenuation of the two low-pass filters used in the disturbance force estimation. This was already predicted when the system was described and analyzed. The spectra of the positional errors in Figure 5 b), 6 b) and Figure 7 b) also show that the influence of the ERDOB rises with increasing speed. Thus, the first-order harmonic of the disturbance force was suppressed almost equally well by the RDOB and ERDOB at the speed $v = 0.2\,\mathrm{m/s}$. But at the speed $v = 0.5\,\mathrm{m/s}$, the ERDOB suppresses the first harmonic much better than

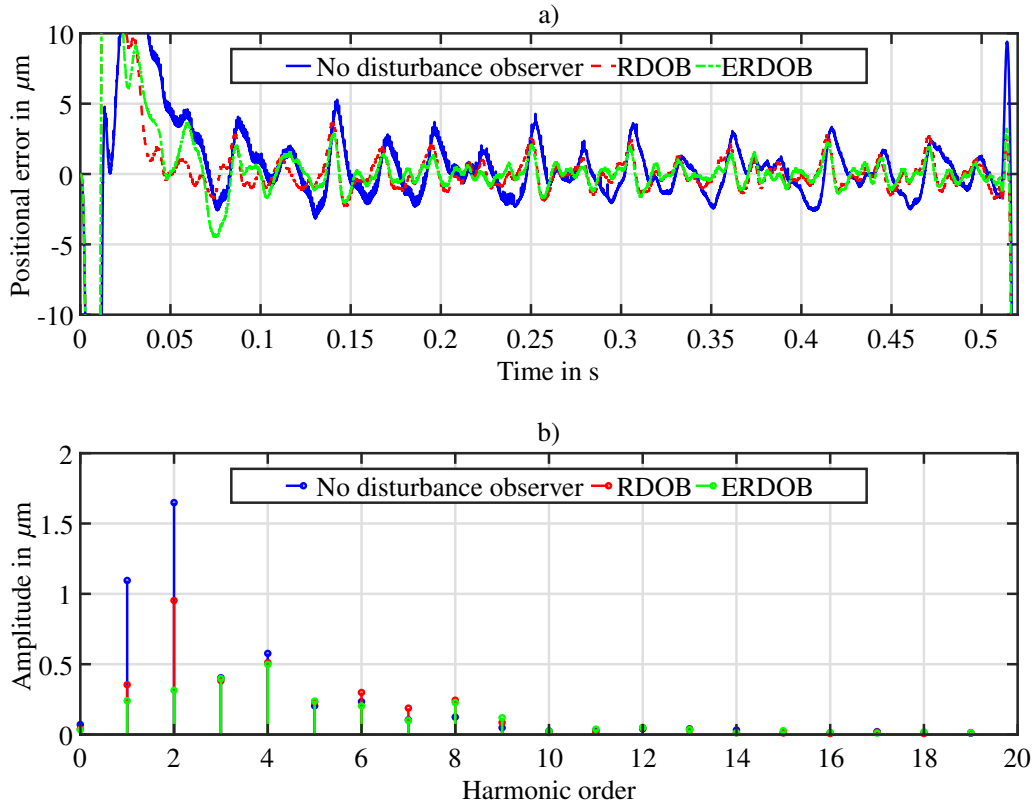

Fig. 6: a) Positional error for $v = 0.2\,\mathrm{m/s}$; b) Positional error frequency characteristic for $v = 0.2\,\mathrm{m/s}$

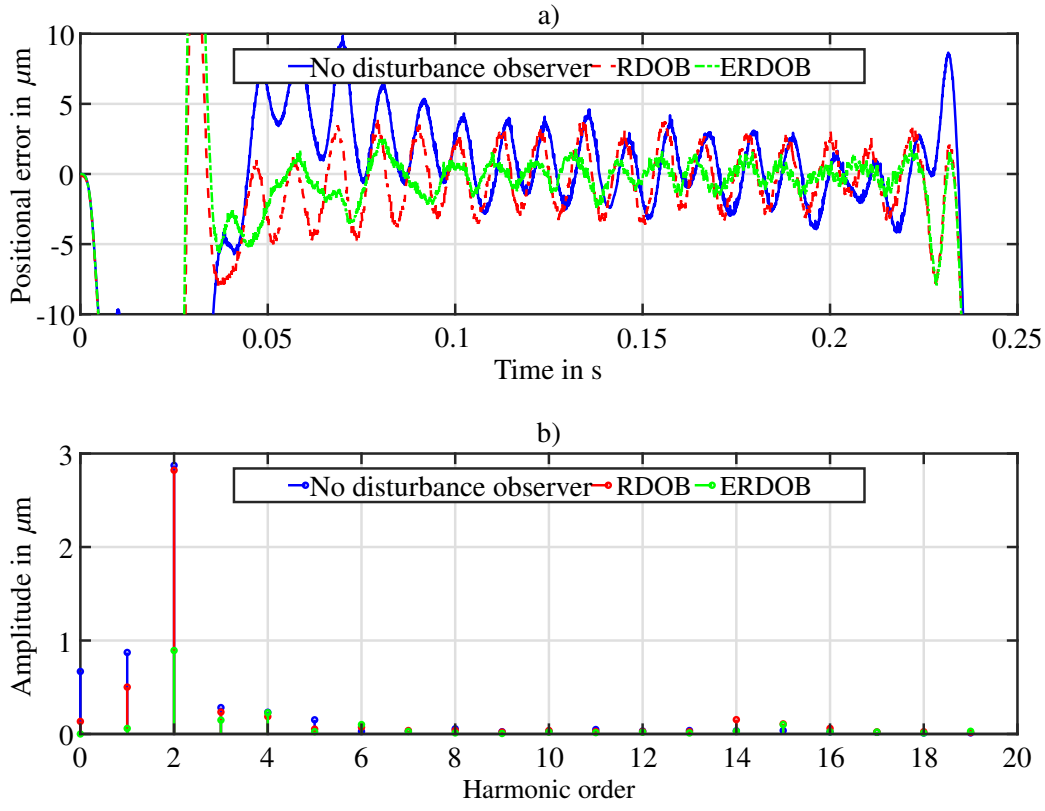

Fig. 7: a) Positional error for $v = 0.5\,\mathrm{m/s}$; b) Positional error frequency characteristic for $v = 0.5\,\mathrm{m/s}$

the RDOB. For the second-rder harmonic, the RDOB has already reached its limit and is no longer able to reduce the impact of this. However, the ERDOB is still able to reduce the impact of the second-order harmonic on the positional error. In summary, this section has shown that an improvement in positional accuracy can be achieved using the concept of ERDOB.

Conclusion

In this paper, the use of an ERDOB for motion control of a PMSLM has been demonstrated. The ability to feed forward dominant harmonics of the cogging force with correct phase positons has reduced the positional error significantly. Also, taking account of all other spectral components of the cogging force with the RDOB has further improved the system in terms of positional accuracy. Therefore, it is to achieve a sufficiently satisfying result possible without any design changes and with little modeling effort. The use of a feedforward structure has the consequence that the feedback controller can be designed with more emphasis on robustness. A further improvement of the system can still be achieved if, in addition to the phase position, the damping of the harmonic caused by the RDOB is also compensated.

References

[1] H.-H. Mu, Y.-F. Zhou, X. Wen, Y.-H. Zhou: “Calibration and compensation of cogging effect in a permanent magnet linear motor”, Mechatronics Vol 19, 2009, pp. 577-585

[2] Hans Butler: “Position Control in Lithographic Equipment [Applications of Control]” PIEEE Control Systems Magazine, 2011, pp. 28-47

[3] P. Van Den Braembussche, J.Swevers, H.Van Brussel, P.Vanherck: “Accurate tracking control of linear synchronous motor machine tool axes”, Mechatronics Vol 6, 1996, pp. 507-521

[4] G. Otten, T. J. A. de Vries, J. van Amerongen, A. M. Rankers, and E. W. Gaal: “Linear motor motion control using a learning feedforward controller”, IEEE/ASME Trans. Mechatronics Vol 2, 1997, pp. 161-170

[5] K. K. Tan, T. H. Lee, H. F. Dou, S. J. Chin, and S. Zhao, “Precision motion control with disturbance observer for pulsewidth-modulated-driven permanent-magnet linear motors”, IEEE Transactions on Magnetics, 2003, Vol 39, pp. 1813-1818

[6] F. Xuewei, Y. Xiaofeng, C. Zhenyu: “A New Linear Motor Force Ripple Compensation Method Based on Inverse Model Iterative Learning and Robust Disturbance Observer”, Complexity Vol 2018, pp. 1-19

[7] D. Schroeder, Martin Buss: “Intelligente Verfahren”, Berlin; Heidelberg: Springer Vieweg, 2017

[8] J. Malaiz, J. Lvine: “An Observer-based design for cogging forces cancellation in permanent magnet linear motors”, Proceedings of the 48h IEEE Conference on Decision and Control (CDC) held jointly with 2009 28th Chinese Control Conference, 2009, pp. 6811-6816

[9] M. Bolderman, M. Lazar and H. Butler, “PhysicsGuided Neural Networks for Inversionbased Feedforward Control applied to Linear Motors”, 2021 IEEE Conference on Control Technology and Applications (CCTA), 2021, pp. 1115-1120

[10] X. Zhang, T. Zhao and X. Gui, “Force Ripple Suppression of Permanent Magnet Linear Synchronous Motor Based on Fuzzy Adaptive Kalman Filter”, 2021 13th International Symposium on Linear Drives for Industry Applications (LDIA), 2021, pp. 1-5